The Effect of Simulator Motion on Pilot Control Behaviour for Agile and Inert Helicopter Dynamics

Frank M. Nieuwenhuizen [1], Peter M.T. Zaal [2],
Harald J. Teufel [1], Max Mulder [2], and Heinrich H. Bülthoff [1]

[1] *Max Planck Institute for Biological Cybernetics, Tübingen, Germany*
(frank.nieuwenhuizen, harald.teufel, heinrich.buelthoff)@tuebingen.mpg.de

[2] *Delft University of Technology, Delft, The Netherlands*
(p.m.t.zaal, m.mulder)@tudelft.nl

Abstract

Even though simulators are often used in flight training, the effects of the different motion components on pilot performance and control behaviour are still not fully understood. In most hexapod motion base simulators the translational motion needs to be reduced significantly to fit within the limited motion space, while the rotational motion might not need attenuation. This paper presents the results of an experiment that investigated the effects of simulator motion in a roll-lateral helicopter control task for both agile and inert helicopter dynamics. The experiment was performed in the MPI Motion Simulator, which has the unique ability of presenting the motion in this task 1-to-1. The results indicate that both roll and lateral motion are important for increasing performance in reducing the roll error. The lateral motion also significantly reduced the lateral tracking errors. Pilots increased their control activity, but had a lower performance in reducing the lateral error for the inert helicopter dynamics. These effects in performance and control activity were caused by a change in the pilots' control strategy as was observed from the multimodal pilot model parameters. The effects on pilot tracking performance were also apparent from a significant change in the disturbance and target open-loop characteristics.

1. INTRODUCTION

In the past decades, flight simulators have been introduced as a training tool for prospective pilots and as important research equipment, for example, for evaluation of the effects of motion cues in manual control tasks. Although there is no consensus about the need for simulator motion for training [1], active control experiments with pilots in the loop have shown favourable effects of simulator motion [2, 3].

In studies on manual control and in most research in aircraft, focus has mainly been put on the rotational degrees of freedom. Various papers have been published on the influence of motion cues in roll control tasks [3–6], pitch control tasks [7–9], and yaw control tasks [10–13]. However, in actual flight, rotational motion is almost always accompanied by linear motion. An example is helicopter hover flight, where roll motion directly results in lateral motion through tilting of the lift vector.

Flight simulators, in general, do not have sufficient capabilities for linear travel as most are based on hexapod motion systems. To reduce the linear simulator travel, two methods are generally used [11]. The first method entails reducing the rotational angles of the motion platform relative to the visual scene, also reducing the required linear simulator motion. In the second method, only the linear cues are scaled such that they can be reproduced by the motion platform. In the first case, all motion cues are different from the visual scene, but still coordinated. In the second case, the motion is not coordinated any more.

A task in which a large linear motion range is required is a helicopter lateral sidestep manoeuvre. This task was the focus of an experiment performed on the NASA Vertical Motion Simulator in which the effect of simulator motion on pilot performance, workload, and motion perception was investigated [11]. It was found that pilot performance increased with increasing motion gains. More recently, the experiment was repeated on the MPI Motion Simulator at the Max Planck Institute for Biological Cybernetics (MPI), where this task can be simulated without motion filters, and similar results were found [14, 15].

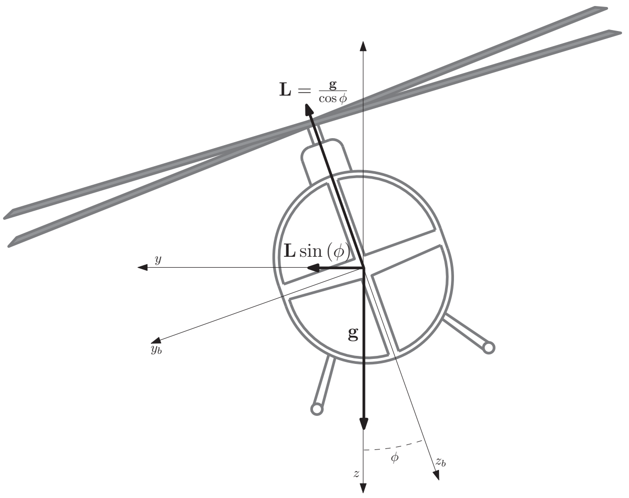

Figure 1: A helicopter in roll-lateral hover.

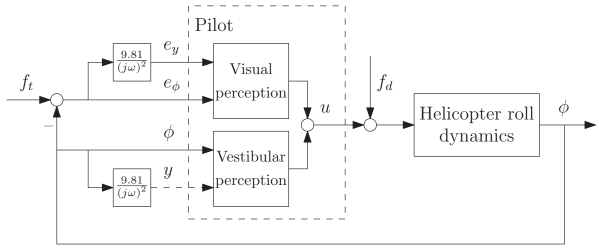

Figure 2: The manual control task.

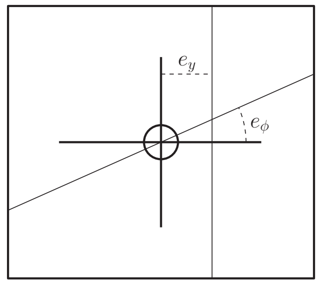

Figure 3: The compensatory display.

These investigations led to a quasi-transfer of training experiment being performed at MPI, where the lateral sidestep manoeuvre was used to investigate the transfer of training between different system dynamics of a simulated helicopter [16]. In this experiment, positive transfer of training was found when switching from agile to inert helicopter dynamics, but not the other way around.

From these investigations it is clear that the role of simulator motion is not yet completely understood. The research described in this paper aims to provide more insight into the effects of motion cues on pilot performance and control behaviour when controlling agile and inert helicopter dynamics in a roll-lateral control task. Pilot identification methods are used to estimate multimodal pilot model parameters to get insight into the underlying perception and control processes of the pilot [17–19].

The paper is structured as follows. First the control task and the motion cues during roll-lateral helicopter hover are introduced. After that, the setup of the experiment and the measurement apparatus will be described. Then, the experimental results of the manual control experiment are reported, followed by a discussion and conclusions.

2. HELICOPTER CONTROL TASK WITH ROLL AND LATERAL MOTION

2.1. Control Task

For simulation of fully coordinated lateral translational helicopter hover flight, roll motion has to be accompanied by lateral platform motion to counteract tilting of the gravity vector with respect to the pilot's head that would result from only rolling the simulator cabin. A schematic representation of a helicopter in roll-lateral flight is presented in Fig. 1. The helicopter has a roll angle ϕ, which causes the lift vector to tilt. The lateral helicopter acceleration equals $\mathrm{L} \cdot \sin(\phi)$.

To quantify the importance of roll and lateral motion in helicopter flight, their effects on manual control behaviour will be evaluated in a manual closed-loop control task, which is depicted in Fig. 2. In this combined target-following disturbance-rejection task the pilot has to actively control the helicopter system dynamics to track a target signal f_t displayed on a compensatory display while compensating for a disturbance f_d on the helicopter dynamics. The independent deterministic signals f_t and f_d allow for identification of visual and physical motion frequency response functions for pilot behaviour.

The signal f_t is equivalent to target helicopter with coordinated roll and lateral motion. The objective of the participants was to follow this target helicopter. A compensatory display, see Fig. 3, showed the roll error e_ϕ, which is the difference between a target f_t and the helicopter roll angle ϕ. Because of the coordinated motion of the target, an error in tracking the roll movement of the target resulted in a coordinated lateral tracking error. The scaled lateral error e_y was also displayed on the screen. The primary task of the participants was to minimise the roll error e_ϕ, while keeping the lateral error small was a secondary task.

The participant's control signal is given as u. The roll and lateral motion (given as ϕ and y in Fig. 2) are coordinated and correlated with the errors e_ϕ and e_y depicted on the visual display.

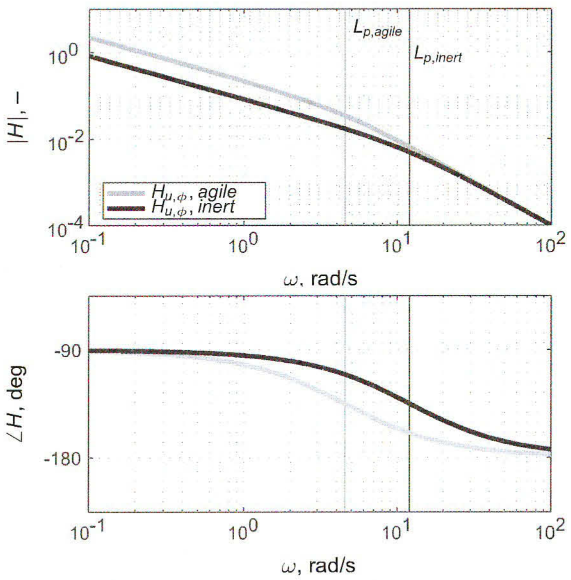

Figure 4: Bode plot of the system dynamics

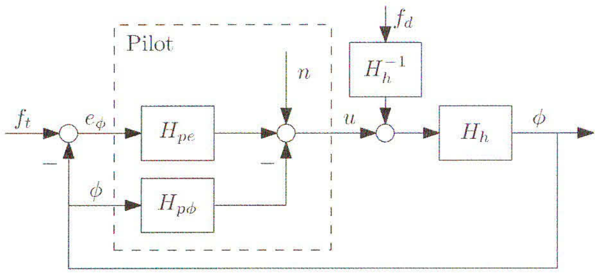

(a) The control loop

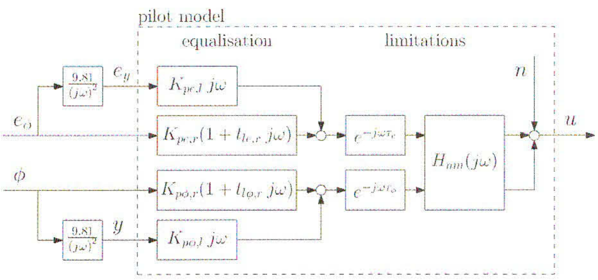

(b) The multimodal pilot model

Figure 5: The control loop and multimodal pilot model.

Quasi-steady flight conditions are assumed for the system dynamics that were controlled by the pilot. The dynamics for the roll motion can be described with a first-order differential form of a rate response type [20]. The lateral motion is fully coordinated with the roll motion. The equations of motion were [11]:

$$\ddot{\phi} = -L_p\dot{\phi} + L_\delta\delta \,, \quad (1)$$

$$\ddot{y} = L\sin(\phi) = g\cdot\tan(\phi) \approx g\cdot\phi \,. \quad (2)$$

The parameter L_p is the roll damping stability derivative and signifies the roll accelerations due to roll rate. In this study, two values were used [16]. The value 4.5 rad/s corresponds to agile dynamics that respond fast to the control inputs of the pilot, the value 12.0 rad/s represents inert dynamics that have higher roll damping and respond sluggish to control inputs. The roll control power L_δ was constant at 2.0 rad/s^2. Parameter g is the gravity constant and equalled 9.81 m/s^2.

The frequency response between the helicopter roll angle ϕ and the pilot input u can be determined from Eq. (1). It is shown in Fig. 4 for the agile and inert dynamics. From the figure it is clear that both dynamics behave as a single integrator at low frequencies. However, for the agile dynamics the break frequency at which the dynamics change to second order behaviour is much lower (at 4.5 rad/s) than for the inert dynamics (at 12.0 rad/s).

The coordinated roll and lateral motion allow the participants to close additional feedback loops in the control task, as shown in Fig. 2, as these motion cues are correlated with the signals e_ϕ and e_y presented on the visual display.

The roll motion is sensed by the semicircular canals. These sensors respond to the roll acceleration $\ddot{\phi}$, but yield a sensation of roll velocity $\dot{\phi}$ [5]. Therefore, providing roll motion in this control task reduces the need for generating visual lead, thus increasing performance.

The lateral acceleration is sensed by the otoliths. These sensors behave as a gain in the frequency range of interest [5], but it is assumed that humans can integrate the otolith output to a sense of lateral velocity [21]. Thus, the otoliths yield an estimate of lateral velocity $\dot{y}$ that is directly related to the roll angle ϕ, see Eq. (2). Therefore, apart from giving additional information for the control of the lateral error e_y, lateral motion also helps to control the roll motion by providing an indirect estimate of the current roll angle ϕ.

2.2. Multimodal Pilot Model

The control task described in the previous section can be modelled as given in Fig. 5a. The control loop consists of the helicopter dynamics H_h, and two pilot response functions H_{pe} and $H_{p\phi}$ that represent the pilot's visual response and response to simulator motion, respectively.

The pilot response functions are represented by the multimodal pilot model given in Fig. 5b. The pilot model consists of gains and time constants, which form the pilot equalisation, and time delays and neuromuscular dynamics, which are the pilot limitations.

Table 1: Forcing function data.

Disturbance, f_d				Target, f_t			
n_d	ω_d	A_d	ϕ_d	n_t	ω_t	A_t	ϕ_t
–	rad s^{-1}	deg	rad	–	rad s^{-1}	deg	rad
5	0.320	1.596	-2.088	6	0.383	0.744	0.537
11	0.703	1.297	1.238	13	0.831	0.567	1.649
23	1.470	0.728	-3.895	27	1.726	0.288	5.033
37	2.365	0.392	3.138	41	2.621	0.161	0.184
51	3.388	0.227	-2.807	53	3.643	0.097	5.836
71	4.666	0.139	-1.808	73	4.858	0.062	4.589
101	6.456	0.087	-1.563	103	6.583	0.040	3.070
137	8.756	0.060	-2.953	139	8.884	0.028	3.635
171	12.208	0.044	-2.626	194	12.400	0.021	1.491
226	17.193	0.035	0.864	229	17.321	0.017	2.883

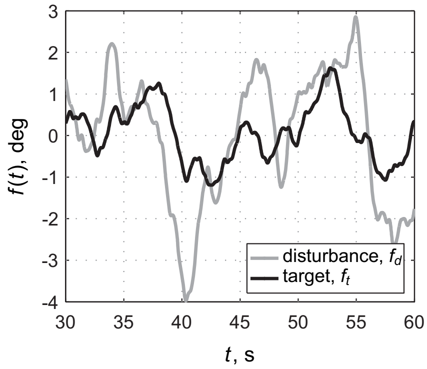

Figure 6: Time histories of disturbance and target forcing functions.

The pilot model has two inputs: e_ϕ and ϕ. The lateral error e_y and position y can be calculated from these inputs by using Eq. (2). The pilot equalisation for both inputs consists of two parts. The first part relates the lateral cues e_y and y to the pilot control signal u, and includes gains $K_{pe,l}$ and $K_{p\phi,l}$, respectively. The second part of the pilot equalisation for both inputs relates the rotational cues e_ϕ and ϕ to the pilot control signal. The channel for e_ϕ includes a gain $K_{pe,r}$ and a lead time constant $t_{le,r}$. The channel for ϕ also includes a gain and lead time constant, $K_{p\phi,r}$ and $t_{l\phi,r}$, respectively.

The pilot limitations in Fig. 5b include the visual time delay τ_e and the motion time delay τ_ϕ, and the pilot neuromuscular dynamics H_{nm}. The neuromuscular dynamics are given by:

$$(3) \qquad H_{nm}(j\omega) = \frac{\omega_{nm}^2}{\omega_{nm}^2 + 2\zeta_{nm}\omega_{nm}j\omega + (j\omega)^2} \, ,$$

with ζ_{nm} and ω_{nm} the neuromuscular damping and frequency, respectively.

The open-loop response functions of the control loop shown in Fig. 5a can be determined for inputs f_d and f_t. These are given as:

$$(4) \qquad H_{ol,d} = \left(H_{pe} + H_{p\phi}\right) H_h \, ,$$

$$(5) \qquad H_{ol,t} = \frac{H_{pe} H_h}{1 + H_{p\phi} H_h} \, .$$

From $H_{ol,d}$ and $H_{ol,t}$, one can determine the crossover frequencies $\omega_{c,d}$ and $\omega_{c,t}$, which are indicators for performance, and phase margins $\varphi_{m,d}$ and $\varphi_{m,t}$, that are a measure for the stability of the control loop.

3. EXPERIMENT SETUP

To investigate the role of roll and lateral motion in a helicopter roll control task for both inert and agile helicopter dynamics, a human-in-the-loop experiment was performed on the MPI Motion Simulator at the Max Planck Institute for Biological Cybernetics [22].

3.1. Method

3.1.1. Forcing Functions

Both a target and a disturbance forcing function were inserted into the control loop to excite the combined pilot-helicopter system, see Fig. 2. In the resulting target-following disturbance-rejection roll-lateral control task, multi-sine forcing functions were used, as their random appearance induces skill-based pilot control behaviour, while giving the experimenter control of the exact properties of the signals in the frequency domain. The forcing functions were calculated according to:

$$(6) \qquad f_{d,t} = \sum_{k=1}^{N_{d,t}} A_{d,t}(k) \sin\left(\omega_{d,t}(k)t + \phi(k)\right) ,$$

where d and t represent the disturbance and target forcing function, respectively. The frequency of the k^{th} sine wave is given by ω, A is the amplitude, and ϕ is the phase. Both forcing functions consisted of N = 10 individual sine waves.

The frequencies of the sine waves are based on previous research [23] and span the frequency range of interest, that is, the frequency range up to where humans actively control the system dynamics. The measurement time of an individual measurement run was T_m = 98.3 seconds. The frequencies were all inte-

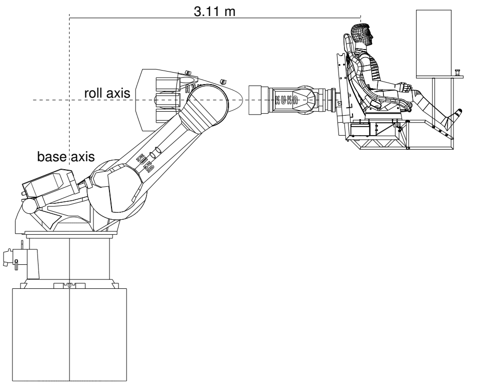

Figure 7: The configuration of the simulator.

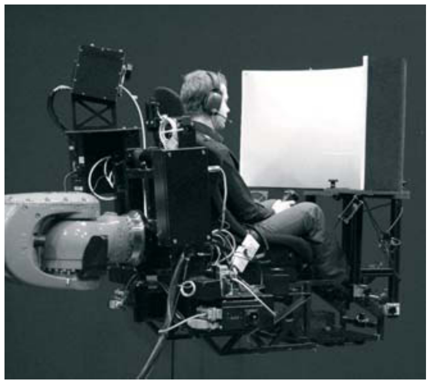

Figure 8: The MPI Motion Simulator.

ger multiples $n_{d,t}$ of the measurement time base frequency, $\omega_m = 2\pi/T_m = 0.0639$ rad/s.

The amplitudes of the sine waves are determined by the following second-order filter:

$$A_{d,t} = \left| \frac{(1 + 0.1j\omega_{d,t})}{(1 + 0.8j\omega_{d,t})} \right| . \quad (7)$$

This second-order low-pass filter reduces the amplitudes at higher frequencies and ensures that the task is not overly difficult. Next, the disturbance and target forcing function amplitudes were scaled to yield forcing function variances of 1.6 and 0.4 deg^2, for the disturbance and target signal, respectively. The increased variance for the disturbance signal yields a control task that is mainly a disturbance-rejection task. The phases of the individual sines were determined randomly, but it was made sure that the properties of the resulting signals were favourable, for example, without the presence of excessive peaks.

Finally, as the disturbance signal is attenuated by passing through the controlled dynamics, the disturbance forcing function is prefiltered with the inverse of the helicopter dynamics appropriate for the experimental condition (see Fig. 5a). Table 1 contains the characteristics of the 10 sine waves of the disturbance and target forcing function, and Fig. 6 shows the resulting time-domain signals.

Table 2: Experimental conditions.

Condition	L_p	Lateral motion	Roll motion
C1	4.50	–	–
C2	4.50	+	–
C3	4.50	–	+
C4	4.50	+	+
C5	12.0	–	–
C6	12.0	+	–
C7	12.0	–	+
C8	12.0	+	+

3.1.2. Independent Variables

Three independent variables were varied in the experiment. To investigate the influence of roll rotational and lateral motion on pilot performance and control behaviour, the roll and lateral motion resulting from the helicopter dynamics could be either on or off. Furthermore, two types of helicopter dynamics were used to investigate if the use of the different motion cues was affected by the agility of the controlled helicopter dynamics. The roll damping stability derivative L_p was either 4.5 or 12.0, representing agile or inert helicopter dynamics, respectively. The experiment had a full factorial design, resulting in the eight experimental conditions given in Table 2.

3.1.3. Apparatus

The experiment was performed on the MPI Motion Simulator [22], which is based on a 3-2-1 serial robot that has 6 degrees of freedom, see Fig. 7. The robot arm has six axes and at the end of the arm a seat is mounted to allow for passive experiments and active human-in-the-loop experiments.

For the current experiment, the axis closest to the simulator seat was used to generate the helicopter roll motion. The back of the middle of the seat is mounted to the axis, resulting in roll motion around the abdomen of the participants. The axis at the base of the simulator was used to generate lateral motion cues by moving the seat along an arc with a radius of 3.11 m, see Fig. 7. At the beginning of each experiment session the simulator seat was moved to a position that allowed for the maximum range of lateral displacement. The large motion space of the simulator allowed the experiment to be performed without motion filters.

Subjects controlled the roll attitude of the helicopter dynamics with a cyclic stick mounted in front of the seat, see Fig. 8. The stick had no breakout force and a low stiffness.

To depict the error e_ϕ between the target f_t and current roll angle ϕ, and the lateral error e_y, a compensatory display was used, given in Fig. 3. The display was projected with a conventional projector on a curved screen. The screen was mounted in front of the simulator seat, 0.7 m in front of the subject, and had an approximate field of view of 90° horizontally by 60° vertically. The location of the display was such that subjects could look at the screen without any rotation of the head.

Subjects wore a headset to communicate with the experimenter and to mask simulator noise. Furthermore, the room where the simulator was located was completely darkened to eliminate any additional visual cues resulting from the static reference frame of the room.

3.1.4. Participants and Instructions

Seven participants took part in the experiment. All were male, with an average age of 25, and were extensively trained on the control task. Before the start of the experiment, the subjects were briefed on the scope of the experiment and the experimental procedure. They were informed of the different experimental conditions given in Table 2. The main instruction to every subject was to minimise the roll error that was displayed on the screen as best as possible. A secondary task was to keep the lateral error small.

3.1.5. Experimental Procedure

During the experiment, five repetitions of each condition were presented randomly. Each trial lasted 110.0 seconds, of which 98.3 seconds were measurement time. The first 11.7 seconds were run-in time to allow subjects to stabilise their control of the helicopter dynamics. Data were logged at a sampling interval of 12 ms.

3.1.6. Dependent Measures

For each run the different signals in the control loop of Fig. 2 were logged. From these measurements a number of dependent measures could be calculated. First, the variance of the error signal e and the pilot control signal u are a measure for pilot tracking performance and control activity, respectively.

The parameters of the pilot model were estimated with a method using Fourier Coefficients [18]. First, the pilot response functions H_{pe} and $H_{p\phi}$ were identified from the signals in the control loop, see Fig. 5a. Then, the parameters of the pilot model were estimated by fitting the pilot model (see Fig. 5b) to the identified response functions. With the pilot model parameters, the open loop response functions $H_{ol,d}$ and $H_{ol,t}$ could be calculated, which were used to determine the cross-over frequencies and phase margins.

3.2. Hypotheses

Motion cues are hypothesised to be more important when controlling the agile helicopter dynamics. This is supported by the fact that the agile helicopter dynamics are equivalent to a double integrator starting at a lower frequency, as compared to the inert dynamics. Double integrator dynamics require the pilot to generate lead, which can be generated visually but also, more efficiently, through vestibular motion perception.

Furthermore, based on previous research [23] it is hypothesised that performance will improve in presence of roll and lateral motion. Roll motion will allow for a better attenuation of the disturbance and an increase in the disturbance crossover frequency. The increased crossover frequency will be caused by an increased overall pilot gain and a decreased time delay.

4. RESULTS

In this section the combined results of seven participants who performed the experiment are given. A repeated measures analysis of variance (ANOVA) was performed to reveal significant trends in the data. First, results for pilot tracking performance and control activity will be presented. Next, the results of the multimodal pilot model identification will be discussed.

4.1. Pilot Performance and Control Activity

The variances of the error signals and the control signal are given in Fig. 9, a measure for pilot tracking performance and control activity, respectively. Conditions C1-C8 are defined in Table 2. Both the error in roll, e_ϕ, and in lateral position, e_y, are given, see Fig. 3. The variances are decomposed into the variances resulting from the input signals of the closed-loop control task given in Fig. 2. The variance components of the forcing functions f_d and f_t are calculated with the power spectral densities of the error and control signals on the input frequencies of the forcing functions [24]. The ANOVA results for pilot performance and control activity are given in Table 3.

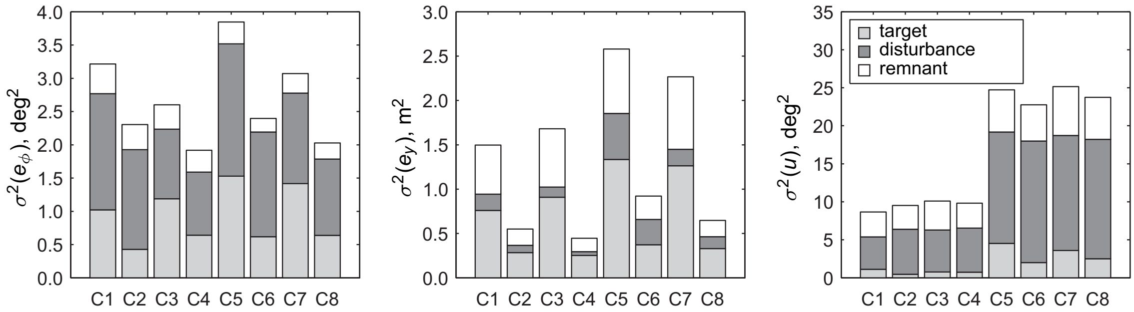

(a) Error signal (b) Lateral error signal (c) Control signal

Figure 9: Variance decomposition of the error and control signals for every condition averaged over seven subjects.

In Fig. 9a, it is shown that roll tracking performance is higher when roll motion is present. This effect is significant as can be observed from Table 3. Lateral motion of the simulator also significantly increases the performance. The performance increase is a result of a reduction in the disturbance variance component (R: F(1,6) = 19.45, $p < 0.01$ and L: F(1,6) = 9.48, $p < 0.05$). This indicates that with either lateral or roll motion pilots could minimise the disturbance on the helicopter dynamics better. In addition, the performance increase is a result of a much better target-tracking performance (reduced magnitude of the target component) for the conditions with lateral motion (L: F(1,6) = 20.96, $p < 0.01$). Thus, one can conclude that in this type of control task, simulator lateral motion is more important to increase performance compared to simulator roll motion.

The remnant variance component in roll tracking performance is significantly lower for the inert helicopter dynamics (D: F(1,6) = 12.98, $p < 0.05$), indicating that pilot behaviour is more linear. From Fig. 9a a small decrease in performance can be noted for the inert helicopter dynamics compared to the agile dynamics (conditions C5-C8 compared to C1-C4), but this effect is not significant. The figure also shows a larger increase in performance, but not significant, when physical motion is available for the inert dynamics compared to the agile dynamics.

Table 3: ANOVA results of the performance and control activity.

Independent Variables		Dependent measures					
		$\sigma^2(e_\phi)$		$\sigma^2(e_y)$		$\sigma^2(u)$	
Factor	df	F	Sig.	F	Sig.	F	Sig.
R	1,6	7.69	$*$	3.48	–	0.49	–
L	1,6	14.89	$**$	35.62	$**$	0.32	–
D	1,6	3.23	–	11.38	$*$	190.61	$**$
R×L	1,6	4.56	–	0.39	–	0.07	–
R×D	1,6	0.10	–	3.15	–	0.03	–
L×D	1,6	3.16	–	3.53	–	1.97	–
R×L×D	1,6	0.50	–	1.28	–	0.63	–

R = roll motion; L = lateral motion; D = helicopter dynamics
$**$ = highly-significant ($p < 0.01$); $*$ = significant ($0.01 \leq p < 0.05$); – = not significant ($p \geq 0.05$)

The variances of the lateral error are given in Fig. 9b. In Table 3 it is shown that the higher performance in lateral error reduction for the conditions with lateral motion is highly significant. Pilots also performed significantly better when controlling the agile helicopter dynamics. The performance increase is a result of the decrease of the disturbance variance component for both roll and lateral motion (R: F(1,6) = 18.60, $p < 0.01$ and L: F(1,6) = 8.64, $p < 0.05$). Furthermore, the disturbance variance component of the lateral error was much smaller when controlling the agile dynamics (D: F(1,6) = 17.90, $p < 0.01$). The target variance component of the lateral error is significantly lower for the conditions with lateral motion (L: F(1,6) = 20.08, $p < 0.01$), and also in this case pilots had a significantly better target-tracking performance when controlling the agile helicopter (D: F(1,6) = 11.67, $p < 0.05$). The remnant variance component was only significantly reduced by lateral motion (L: F(1,6) = 62.29, $p < 0.01$).

From Fig. 9c a large increase in control activity can be seen for the inert helicopter dynamics compared to the agile helicopter dynamics. This result is highly significant, see Table 3. Because of the higher gain of the agile helicopter dynamics at lower frequencies (Fig. 4) the control inputs of the pilot can be smaller in magnitude. Roll and lateral motion did not significantly affect overall control activity. The disturbance component in the control signal was significantly lower for the agile helicopter dynamics (D: F(1,6) = 220.81, $p < 0.01$), and also the target component was significantly lower (D: F(1,6) = 301.07, $p < 0.01$). In addition, the target component in the pilot control signal significantly reduced in the conditions with lateral motion (L: F(1,6) = 14.84, $p < 0.01$). The remnant component is significantly lower for the

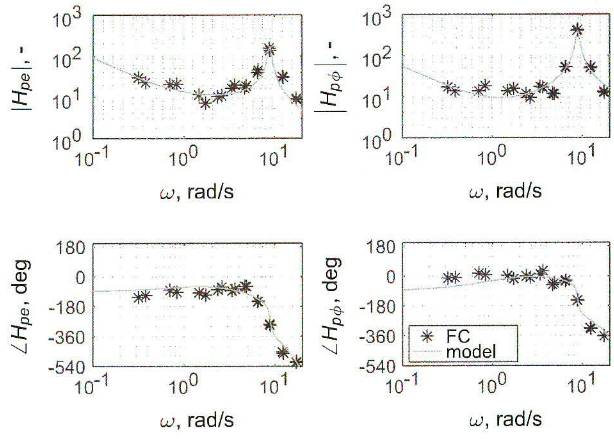

Figure 10: Pilot frequency response function.

agile helicopter dynamics (D: $F(1,6) = 18.11$, $p < 0.01$). The percentage of remnant in the total control signal is approximately two times bigger for the agile helicopter dynamics (40% compared to 20%), indicating that the pilot response is more linear for the inert helicopter dynamics.

4.2. Pilot Control Behaviour

Using the averaged time-domain data of all runs for every condition and subject, the pilot frequency response functions H_{pe} and $H_{p\phi}$ were calculated using Fourier coefficients (FC). Next, the pilot model given in Fig. 5 was fit on the frequency response estimates using a gradient based optimisation [18]. For the conditions without motion, the pilot model only contained the visual perception path H_{pe}. The bode plots of the identified pilot response functions and the estimated pilot model are given in Fig. 10 for C5 of participant 7.

4.2.1. Pilot Model Parameters

The pilot model parameters for the visual perception channel and the neuromuscular dynamics are given in Fig. 11. The corresponding ANOVA data is given in Table 4. The error bars in the figures are corrected for between-subject variability by adjusting the data for the subject means.

As can be observed from Fig. 11a and Table 4, the lateral error perception gain $K_{pe,l}$ is significantly reduced with both roll and lateral motion, tentatively indicating that participants put more emphasis on the motion cues than on the visual cues. In addition, there is a highly significant interaction between roll and lateral motion.

The roll error perception gain $K_{pe,r}$ is significantly re-

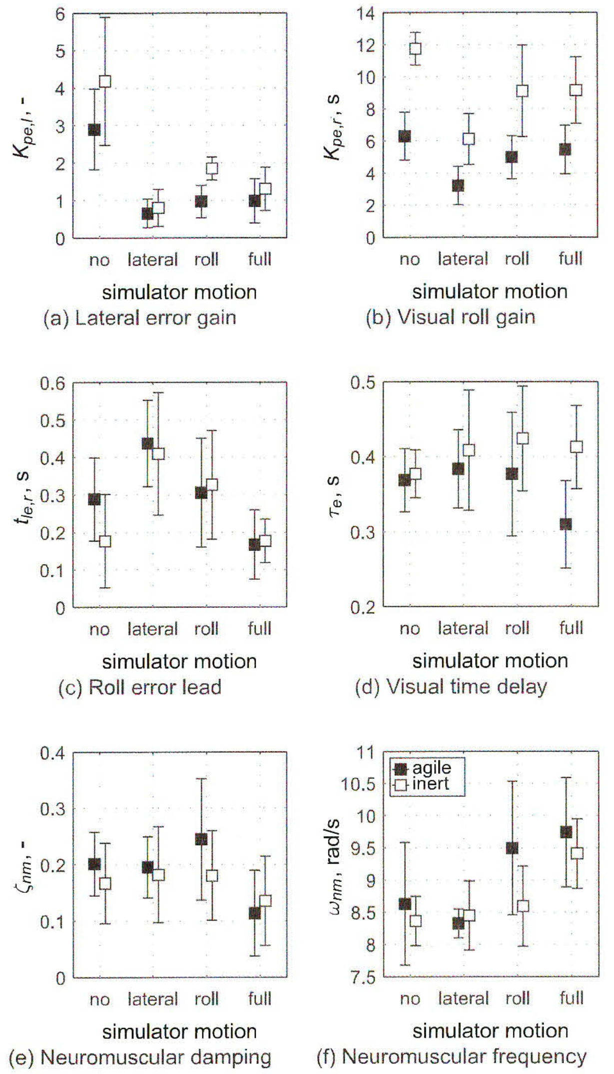

Figure 11: Pilot visual perception channel and neuromuscular dynamics parameters.

duced with lateral motion (Fig. 11b). This might be an indication that lateral motion cues are more beneficial than roll motion cues. Furthermore, the gain is significantly higher for the inert helicopter dynamics. This is in correspondence with the higher control activity for inert helicopter dynamics found in Fig. 9c. The significant interaction between roll and lateral motion is caused by a decrease in the roll error perception gain by lateral motion, while the gain is not decreased if roll motion is present.

For the roll error lead constant $t_{le,r}$ only a significant interaction is found between roll and lateral motion. As can be seen in Fig. 11c, there is a large reduction in visual lead if roll motion is added to a condition with lateral motion. The visual lead is increased if roll motion is added to a condition without lateral motion. The visual perception time delay and neuromuscular

Table 4: ANOVA results of the pilot visual perception channel and neuromuscular dynamics parameters.

Independent Variables		Dependent measures											
		$K_{pe,l}$		$K_{pe,r}$		$t_{le,r}$		τ_e		ζ_{nm}		ω_{nm}	
Factor	df	F	Sig.	F	Sig.	F	Sig.	F	Sig.	F	Sig.	F	Sig.
R	1,6	9.80	*	0.27	–	3.74	–	0.03	–	0.29	–	5.97	*
L	1,6	12.67	*	7.39	*	0.32	–	0.08	–	1.82	–	0.73	–
D	1,6	5.26	–	30.43	**	0.40	–	4.51	–	0.71	–	4.37	–
R×L	1,6	32.26	**	11.91	*	11.58	*	1.48	–	2.95	–	1.57	–
R×D	1,6	0.06	–	0.07	–	0.77	–	3.36	–	0.01	–	4.44	–
L×D	1,6	2.99	–	3.36	–	0.25	–	0.72	–	2.48	–	1.53	–
R×L×D	1,6	0.36	–	3.16	–	0.46	–	0.95	–	0.24	–	0.03	–

R = roll motion ** = highly-significant ($p < 0.01$)
L = lateral motion * = significant ($0.01 \leq p < 0.05$)
D = helicopter dynamics – = not significant ($p \geq 0.05$)

damping were both not significantly affected by any of the independent variables. The neuromuscular frequency was significantly increased if roll motion was available (Fig. 11f), indicative of control over an increased bandwidth. This is also observed in previous experiments [23].

In Fig. 12 and Table 5 the error-bar plots and the ANOVA results are given for the pilot motion perception parameters, respectively. As the motion perception parameters are not defined for the conditions without motion (C1 and C5), the effects of roll and lateral motion can not be analysed separately in an ANOVA. To reveal any significant effects of motion, an ANOVA with three levels of motion (roll, lateral, and roll and lateral motion combined) in addition to the two levels of dynamics was performed.

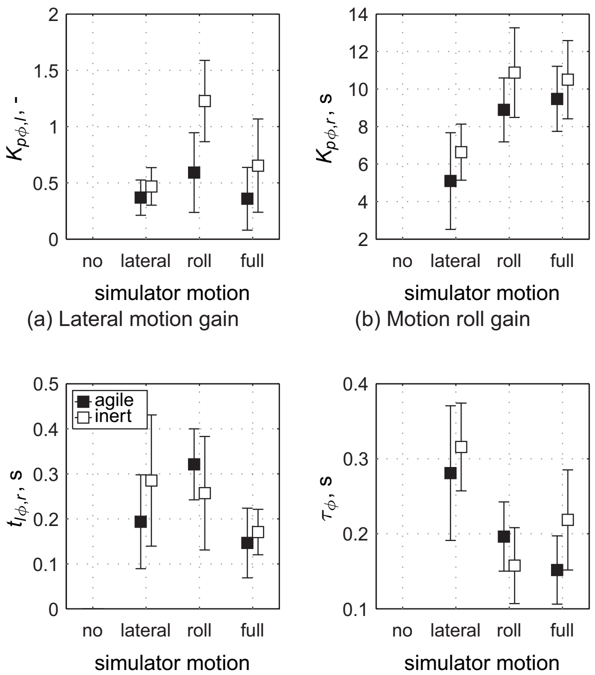

(a) Lateral motion gain (b) Motion roll gain (c) Roll motion lead (d) Motion time delay

Figure 12: Pilot physical motion perception channel parameters.

Table 5: ANOVA results of the pilot physical motion perception channel parameters.

Independent Variables		Dependent measures							
		$K_{p\phi,l}$		$K_{p\phi,r}$		$t_{l\phi,r}$		τ_ϕ	
Factor	df	F	Sig.	F	Sig.	F	Sig.	F	Sig.
M	2,12	4.54	*	6.21	*	3.91	*	28.03	**
D	1,6	4.66	–	10.50	*	0.22	–	0.42	–
M×D	2,12	4.06	*	0.18	–	0.93	–	1.17	–

M = motion ** = highly-significant ($p < 0.01$)
D = helicopter dynamics * = significant ($0.01 \leq p < 0.05$)
– = not significant ($p \geq 0.05$)

The lateral motion perception gain $K_{p\phi,l}$ was significantly affected by the level of motion. In Fig. 12a, it is shown that the lateral motion perception gain is increased for the condition with only roll motion, possibly indicating that participants used the roll motion to estimate lateral motion. The significant interaction is caused by the larger increase for the inert helicopter dynamics, where the sluggish movement necessitates increased reliance on the lateral movement of the helicopter.

The roll motion perception gain $K_{p\phi,r}$ is significantly affected by roll motion. If roll motion is present, the roll motion perception gain is significantly higher (Fig. 12b). Also the increased gain for the inert helicopter dynamics is a significant effect. There is a significantly reduced value for the roll motion perception lead constant for the full motion condition, as can be seen in Fig. 12c, showing that with coordinated roll-lateral simulator motion there is less need for roll velocity. In Fig. 12d, it is shown that the motion perception time delay is significantly reduced for the conditions with roll motion, tentatively indicating that cues for the inner roll control loop allow for faster processing.

4.2.2. Open-Loop Response Functions

The crossover frequencies and phase margins of the disturbance and target open-loop response functions are performance and stability characteristics for attenuation of the disturbance and the target signal.

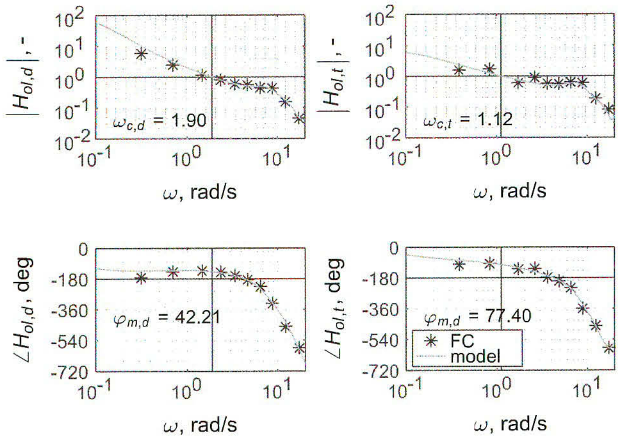

Figure 13: Open-loop response functions.

They are determined from the open-loop response functions. An example is given in Fig. 13 for C3 of participant 4. The disturbance and target open loop crossover frequencies and phase margins are given in Fig. 14. The ANOVA results are given in Table 6.

The disturbance crossover frequency $\omega_{c,d}$ is significantly higher if roll motion or lateral motion are available. This increased disturbance crossover frequency for conditions with physical motion is commonly observed in other experiments [3, 23]. The interaction between roll and lateral motion is caused by the larger increase of the disturbance crossover frequency for roll motion if lateral motion is not available, as compared to when lateral motion is also available. This is an indication that providing motion cues for the inner roll control loop increases the control bandwidth in this task. The disturbance crossover frequency is also higher for the conditions with agile helicopter dynamics, see Fig. 14a. The effect of the increase in disturbance crossover frequency is a decrease in disturbance phase margin as can be observed in Fig. 14c.

The target crossover frequency is significantly reduced when roll and lateral motion are present, see

Table 6: ANOVA results of the crossover frequencies and phase margins.

Independent Variables		Dependent measures							
		$\omega_{c,d}$		$\omega_{c,t}$		$\varphi_{m,d}$		$\varphi_{m,t}$	
Factor	df	F	Sig.	F	Sig.	F	Sig.	F	Sig.
R	1,6	8.43	*	42.86	**	2.54	–	61.35	**
L	1,6	6.59	*	6.14	*	4.08	–	6.85	*
D	1,6	102.70	**	48.15	**	28.74	**	1.65	–
R×L	1,6	16.15	**	61.00	**	2.90	–	2.47	–
R×D	1,6	4.70	–	18.99	**	0.18	–	0.11	–
L×D	1,6	0.77	–	16.27	**	0.81	–	9.94	*
R×L×D	1,6	3.02	–	48.50	**	6.59	*	29.00	**

R = roll motion
L = lateral motion
D = helicopter dynamics

** = highly-significant ($p < 0.01$)
* = significant ($0.01 \leq p < 0.05$)
– = not significant ($p \geq 0.05$)

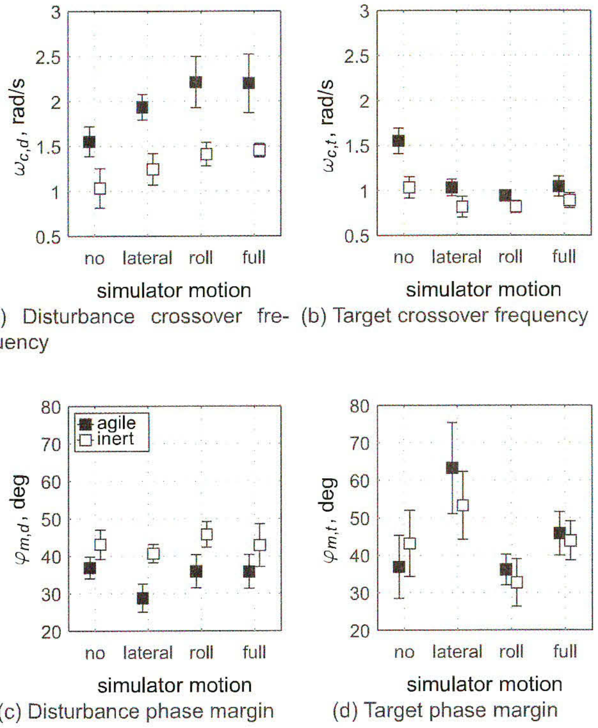

(a) Disturbance crossover frequency (b) Target crossover frequency (c) Disturbance phase margin (d) Target phase margin

Figure 14: Crossover frequencies and phase margins.

Fig. 14b. The decrease in target crossover frequency for roll without lateral motion and the increase with lateral motion is a significant interaction effect. The target crossover frequency is significantly lower for the inert helicopter dynamics. The interactions between dynamics and roll or lateral motion indicate a larger decrease in target crossover frequency due to roll or lateral motion for the agile dynamics compared to the inert dynamics. There is a significant increase in the target phase margin when lateral motion is available, but a significant decrease when roll motion is present. As indicated in Fig. 14d, the target phase margin is increased more for agile dynamics compared to the inert dynamics if lateral motion is available, as observed from the interaction between the dynamics and lateral motion.

5. DISCUSSION

The experiment investigated the effects of simulator roll and lateral motion in a roll-lateral target-following disturbance-rejection control task. The effects of these motion components were examined for agile and inert helicopter dynamics.

By providing simulator roll motion, participants were able to significantly increase performance in reducing the roll error in the control task. This was mainly due to a reduction in the disturbance variance component in the error signals. The simulator lateral motion allowed for an increase in performance in reducing the roll error. Furthermore, lateral error could be reduced with higher performance when lateral motion was available to the participants. Participants showed that they were better at rejecting the disturbance and following the target, as a reduction in the disturbance variance component, as well as in the target variance component were found. This implies that, for this type of control task, lateral motion is more important for increasing overall performance.

Supplying participants with roll and lateral motion resulted in a change in the control strategy of the pilot as was seen by significant changes in the multimodal pilot model parameters. Supplying motion cues in the control task resulted in a shift from reliance on the error perception to reliance on simulator motion. When roll motion was present, participants showed control over a higher bandwidth and decreased processing times.

The change in control strategy was also seen by an increase in the disturbance crossover frequency with both roll and lateral motion, indicating a higher performance in reducing the disturbance error. Furthermore, the target crossover frequency reduced with both motion components and the target phase margin increased. These effects are also observed in previous research investigating the effects of motion on pilot control behaviour [3].

The helicopter dynamics did not have an influence on the roll error in this task, but did show a significant effect on the lateral error and the pilot control activity. When the dynamics were more inert, participants needed larger control inputs to perform the task, and showed worse performance in lateral error compared to the agile dynamics. For inert helicopter dynamics, the roll error perception gain and the roll motion perception gain significantly increased, resulting in a higher control activity.

For the agile helicopter dynamics the disturbance crossover frequency was significantly higher, and the disturbance phase margin was significantly lower, indicating increased performance and lower stability. The target crossover frequency was also significantly higher with agile helicopter dynamics.

In this experiment, participants performed a roll-lateral target-following disturbance-rejection control task. The disturbance-task was made dominant by reducing the power of the target forcing function. In previous experiments it was shown that pilot control behaviour is significantly affected by the type of task and the power of the individual forcing functions [25]. It should therefore be noted that the results found in the current study apply to the task used in this experiment.

Furthermore, the display used in the experiment is a compensatory display, which only gives information on the error between the desired and current roll angle, and the desired and current lateral position. By using a compensatory display, the visual cues that may be perceived from the display are reduced, allowing for the proper modelling of multimodal pilot control behaviour. Also, the use of a compensatory display allows for a comparison of the results to results from many previous experiments, as most work in pilot modelling was performed using this type of display. In most real helicopter operations, however, the visual information also contains attitude information, possibly making the use of a pursuit display more appropriate.

The visual display presented two errors to the pilots (roll and lateral). Although this multi-axis control task is in accordance with many real helicopter tasks (for example, hovering to a target location while reducing disturbances in roll), in many previous experiments on the identification of multimodal pilot control behaviour only a single error was visible on the display. This should be taken into account when comparing the results to previous experiments. The two errors may have increased pilot workload. In addition, although the two errors resulted from the same target signal, pilots may have controlled the two errors independently in small intervals of time. More research is needed on the use of pursuit displays and multi-axis tasks in human control experiments.

The MPI Motion Simulator is unique in that it can produce large linear motion at the pilot station. For most conventional hexapod motion base simulators, the simulation of large linear accelerations is difficult and motion filters need to be used to attenuate the helicopter motion to fit the limited simulator motion space. These motion filters are known to significantly affect pilot control behaviour. In the current experiment on the MPI Motion Simulator, lateral motion could be presented 1-to-1, that is, without any motion filters. However, to produce the lateral motion at the pilot station, the pilot seat moved along an arc. This introduced longitudinal accelerations, which are normally not present in a roll-lateral task, possibly affecting the results.

6. CONCLUSIONS

This paper presented an investigation into the effects of roll and lateral motion with agile and inert helicopter dynamics. Pilot performance and control behaviour was measured in a roll-lateral target-following disturbance-rejection control task. The experiment was performed on the MPI Motion Simulator without any motion filtering, as the simulator was capable of performing large linear motion at the pilot station.

The results indicate that overall pilot performance was significantly increased by roll and lateral motion, but the increase is more significant with lateral motion. The lateral error could be minimised more effectively for the agile helicopter dynamics. This was also apparent from the disturbance and target crossover frequencies and phase margins.

Pilot control activity was significantly higher for the inert helicopter dynamics, but the effect of roll and lateral motion was found to be similar for both types of helicopter dynamics.

The changes in pilot performance and control activity were the result of a significant change in pilot control behaviour and indicate that in a roll-lateral helicopter control task both roll and lateral motion are important to accurately perform the task. This warrants the use of flight simulators that can accurately reproduce the large lateral motion of a helicopter.

REFERENCES

[1] Bürki-Cohen, J., Soja, N. N., and Longridge, T., "Simulator Platform Motion - The Need Revisited," *The International Journal of Aviation Psychology*, Vol. 8, No. 3, 1998, pp. 293–317.

[2] Zaal, P. M. T., Nieuwenhuizen, F. M., Mulder, M., and Van Paassen, M. M., "Perception of Visual and Motion Cues During Control of Self-Motion in Optic Flow Environments," *Proceedings of the AIAA Modeling and Simulation Technologies Conference and Exhibit, Keystone (CO)*, No. AIAA-2006-6627, 21–24 Aug. 2006.

[3] Pool, D. M., Mulder, M., Van Paassen, M. M., and Van der Vaart, J. C., "Effects of Peripheral Visual and Physical Motion Cues in Roll-Axis Tracking Tasks," *Journal of Guidance, Control, and Dynamics*, Vol. 31, No. 6, Nov.–Dec. 2008, pp. 1608–1622.

[4] Stapleford, R. L., Peters, R. A., and Alex, F. R., "Experiments and a Model for Pilot Dynamics with Visual and Motion Inputs," NASA Contractor Report NASA CR-1325, NASA, 1969.

[5] Hosman, R. J. A. W., *Pilot's perception and control of aircraft motions*, Doctoral dissertation, Faculty of Aerospace Engineering, Delft University of Technology, 1996.

[6] Van der Vaart, J. C., *Modelling of Perception and Action in Compensatory Manual Control Tasks*, Doctoral dissertation, Faculty of Aerospace Engineering, Delft University of Technology, 1992.

[7] Van Gool, M. F. C. and Mooij, H. A., "A Comparison of In-Flight and Ground-Based Pitch Attitude Tracking Experiments," *Proceedings of the Twelfth Annual Conference on Manual Control*, University of Illinois, Urbana (IL), May 25–27 1976, pp. 443–454.

[8] Steurs, M., Mulder, M., and Van Paassen, M. M., "A Cybernetic Approach to Assess Flight Simulator Fidelity," *Proceedings of the AIAA Modelling and Simulation Technologies Conference and Exhibit, Providence (RI)*, No. AIAA-2004-5442, 16–19 Aug. 2004.

[9] Dehouck, T. L., Mulder, M., and Van Paassen, M. M., "The Effects of Simulator Motion Filter Settings on Pilot Manual Control Behaviour," *Proceedings of the AIAA Modeling and Simulation Technologies Conference and Exhibit, Keystone (CO)*, No. AIAA-2006-6250, 21–24 Aug. 2006.

[10] Zacharias, G. and Young, L., "Influence of Combined Visual and Vestibular Cues on Human Perception and Control of Horizontal Rotation," *Experimental Brain Research*, Vol. 41, No. 9, Jan. 1981, pp. 159–171.

[11] Schroeder, J. A., "Helicopter Flight Simulation Motion Platform Requirements," Tech. Rep. NASA/TP-1999-208766, NASA, July 1999.

[12] Grant, P. R., Yam, B., Hosman, R., and Schroeder, J. A., "Effect of Simulator Motion on Pilot Behavior and Perception," *Journal of Aircraft*, Vol. 43, No. 6, Nov. – Dec. 2006, pp. 1914–1924.

[13] Ellerbroek, J., Stroosma, O., Mulder, M., and Van Paassen, M. M., "Role Identification of Yaw and Sway Motion in Helicopter Yaw Control Tasks," *Journal of Aircraft*, Vol. 45, No. 4, July–Aug. 2008, pp. 1275–1289.

[14] Beykirch, K., Nieuwenhuizen, F. M., Teufel, H. J., Nusseck, H.-G., Butler, J. S., and Bülthoff, H. H., "Control of a Lateral Helicopter Side-step Maneuver on an Anthropomorphic Robot," *Proceedings of the AIAA Modeling and Simulation Technologies Conference and Exhibit, Hilton Head (SC)*, No. AIAA-2007-6801, 20–23 Aug. 2007.

[15] Beykirch, K. A., Nieuwenhuizen, F. M., Teufel, H. J., Nusseck, H.-G., and Bülthoff, H. H., "A Roll-Lateral Helicopter Side-Step Maneuver on the MPI Motion Simulator," *Proceedings of the AHS 64th Annual Forum and Technology Display*, apr 2008.

[16] Nusseck, H.-G., Teufel, H. J., Nieuwenhuizen, F. M., and Bülthoff, H. H., "Learning System Dynamics: Transfer of Training in a Helicopter Hover Simulator," *Proceedings of the AIAA Modeling and Simulation Technologies Conference and Exhibit, Honolulu (HI)*, No. AIAA-2008-7101, 18–21 Aug. 2008.

[17] Nieuwenhuizen, F. M., Beykirch, K. A., Mulder, M., and Bülthoff, H. H., "Identification of Pilot Control Behavior in a Roll-Lateral Helicopter Hover Task," *Proceedings of the AIAA Modeling and Simulation Technologies Conference and Exhibit, Hilton Head (SC)*, No. AIAA-2007-6799, 20–23 Aug. 2007.

[18] Nieuwenhuizen, F. M., Zaal, P. M. T., Mulder, M., Van Paassen, M. M., and Mulder, J. A., "Modeling Human Multichannel Perception and Control Using Linear Time-Invariant Models," *Journal of Guidance, Control, and Dynamics*, Vol. 31, No. 4, July–Aug. 2008, pp. 999–1013.

[19] Zaal, P. M. T., Pool, D. M., Mulder, M., and Van Paassen, M. M., "New Types of Target Inputs for Multi-Modal Pilot Model Identification," *Proceedings of the AIAA Modeling and Simulation Technologies Conference and Exhibit, Honolulu (HI)*, No. AIAA-2008-7106, 18–21 Aug. 2008.

[20] Padfield, G. D., *Helicopter Flight Dynamics*, American Institute of Aeronautics and Astronautics, Inc., 1801 Alexander Bell Drive, Reston, VA, 2nd ed., 2007.

[21] Van der Steen, H., *Self-Motion Perception*, Doctoral dissertation, Faculty of Aerospace Engineering, Delft University of Technology, 1998.

[22] Teufel, H. J., Nusseck, H.-G., Beykirch, K. A., Bulter, J. S., Kerger, M., and Bülthoff, H. H., "MPI Motion Simulator: Development and Analysis of a Novel Motion Simulator," *Proceedings of the AIAA Modeling and Simulation Technologies Conference and Exhibit, Hilton Head (SC)*, No. AIAA-2007-6476, 20–23 Aug. 2007.

[23] Zaal, P. M. T., Pool, D. M., De Bruin, J., Mulder, M., and Van Paassen, M. M., "Use of Pitch and Heave Motion Cues in a Pitch Control Task," *Journal of Guidance, Control, and Dynamics*, Vol. 32, No. 2, March–April 2009, pp. 366–377.

[24] Jex, H. R. and Magdaleno, R. E., "Roll Tracking Effects of G-vector Tilt and Various Types of Motion Washout," *Fourteenth Annual Conference on Manual Control*, University of Southern California, Los Angeles (CA), April 25–27 1978, pp. 463–502.

[25] Zaal, P. M. T., Pool, D. M., Chu, Q. P., Van Paassen, M. M., Mulder, M., and Mulder, J. A., "Modeling Human Multimodal Perception and Control Using Genetic Maximum Likelihood Estimation," *Journal of Guidance, Control, and Dynamics*, Vol. 32, No. 4, July–Aug. 2009, pp. 1089–1099.